Defining the *Z–R* Relationship Using Gauge Rainfall with Coarse Temporal Resolution: Implications for Flood Forecasting

Punpim Puttaraksa Mapiam, Ph.D.[1]; Ashish Sharma, Ph.D.[2]; and Nutchanart Sriwongsitanon, Ph.D.[3]

Abstract: This paper demonstrates a procedure for deriving the *Z–R* relationship using poor temporal resolution gauge rainfall data and evaluates its impact on runoff forecasting in the upper Ping River Basin in Northern Thailand. The procedure is based on the use of a scaling logic to modify the *Z–R* relationship calibrated using daily (or other coarse) resolution ground rainfall data. This scaling procedure is demonstrated using daily gauge data and results in radar rainfall estimates that lead to improved runoff simulations and flood forecasts for the upper Ping River Basin compared with the case in which the daily (or raw) *Z–R* relationship is used or even when the daily gauge rainfall is used alone. This evaluation is based on hourly comparisons for the high rainfall season over a period of 3 years (2004–2006) at six point locations in the catchment. This scaling relationship has significant implications for flood modeling in most of the developing world that has weather radar coverage and a daily gauge network but a limited continuous ground rainfall measuring network. **DOI: 10.1061/(ASCE)HE.1943-5584.0000616.**

Author keywords: Radar rainfall; Rain gauge rainfall; Runoff estimation; Scaling.

Introduction

Measured rainfall is a significant input in any hydrological modeling application. Weather radars have developed into viable alternatives to ground-measured rainfall because of their ability to sample in space and time (Seed and Austin 1990; Collinge and Kirby 1987; Sun et al. 2000; Uijlenhoet 2001; Vieux 2003), especially in regions with limited ground rainfall measuring networks (Yang et al. 2004; Segond et al. 2007). A number of studies vouch for the efficacy of radar rainfall for flood estimation and forecasting as an alternative to a sparse or poor ground rain-gauge network (Wyss et al. 1990; Pessoa et al. 1993; Borga et al. 2000; Sun et al. 2000; Morin et al. 2009; Anquetin et al. 2010), although it is considered useful to have a minimal ground rain-gauge network to assist with the specification and update of the radar reflectivity-rainfall relationship (or the *Z–R* relationship) (Chumchean et al. 2006a, b). This paper demonstrates an alternative for specifying the *Z–R* relationship in regions having only daily or coarser resolution ground rainfall data and evaluates the advantages that result when used for flood modeling applications.

Use of a power-law *Z–R* relationship [$Z = AR^b$ where Z is radar reflectivity ($mm^6\ m^{-3}$); R is the rainfall rate ($mm\ h^{-1}$); and A and b are parameters], calibrated against ground rainfall data located within the radar coverage, is the traditional approach for radar rainfall estimation (Battan 1973; Rinehart 1991; Doviak and Zrnic 1992; Collier 1996; Krajewski and Smith 2002).

The conventional approach to specifying the relationship (or the parameters A and b) is to use the gauge rainfall data at the finest resolution available and aggregate the radar rainfall to the same resolution. The resulting *Z–R* relationship is then assumed to be valid for use at other temporal resolutions and is often used to ascertain radar rainfall at much finer resolutions than the available gauge data. This assumption has been put into question by Mapiam et al. (2009), with data from three radar locations and their associated dense rain-gauge networks all pointing to the need for a transformation for the A parameter of the *Z–R* relationship as a function of the time resolution at which the rainfall is to be estimated. Mapiam et al. (2009) goes further and proposes a transformation function for the A parameter of the *Z–R* relationship, which is shown to be stable across the three regions at which it is tested. Although the need for the preceding transformation appears justified when there is a mismatch in the temporal scales at which the *Z–R* relationship is derived and used, its impact on flow estimation has not been previously studied.

The question that arises is whether the aforementioned scaling transformation enables better assessment of peak flow events in a typical catchment and the radar rainfall could be applied for flood forecasting purposes. This paper investigates the relative benefits offered by the use of alternate rainfall estimation methods for simulation of the runoff hydrograph in the upper Ping River Basin, Thailand. Daily gauge rainfall and two products of radar rainfall were specified as inputs to the selected rainfall-runoff model for runoff simulation. The daily gauge rainfall (DGR) was spatially averaged by using the Thiessen polygon approach over the study region to form the first of the evaluated rainfall input alternatives. The first radar rainfall product, the hourly radar rainfall (HRR), was ascertained using the climatological daily *Z–R* relationship proposed by Mapiam and Sriwongsitanon (2008) to convert instantaneous radar reflectivity into radar rainfall intensity, followed by accumulating the instantaneous radar rainfall into hourly radar rainfall by using the algorithm proposed by Fabry et al. (1994).

[1]Dept. of Water Resources Engineering, Faculty of Engineering, Kasetsart Univ., Bangkok 10900, Thailand. E-mail: fengppm@ku.ac.th

[2]Professor, School of Civil and Environmental Engineering, Univ. of New South Wales, Sydney 2052, Australia. E-mail: a.sharma@unsw.edu.au

[3]Associate Professor, Dept. of Water Resources Engineering, Faculty of Engineering, Kasetsart Univ., 50 Paholyothin Rd., Ladyao, Jatujak, Bangkok 10900, Thailand (corresponding author). E-mail: fengnns@ku.ac.th

Note. This manuscript was submitted on July 21, 2011; approved on March 15, 2012; published online on January 20, 2014. Discussion period open until October 22, 2014; separate discussions must be submitted for individual papers. This paper is part of the ***Journal of Hydrologic Engineering***, © ASCE, ISSN 1084-0699/04014003(10)/$25.00.

The second radar rainfall product was formulated by applying the scaled transformation equation introduced by Mapiam et al. (2009) to transform the daily A parameter of the Z–R relationship to an hourly Z–R relationship. The hourly scale-transformed Z–R relationship was then used to calculate hourly radar rainfall (HRRS). The DGR, HRR, and HRRS were used as the three alternative rainfall inputs to the catchment simulation model for hourly flow estimation at six runoff stations in the study area. For ease of comparison across the various methods, the DGR was assessed at hourly time steps by considering hourly rain depths equal to 1/24 of the daily rainfall before inputting into the hydrological model. A summary of the rationale behind the three data sets, along with the benefits and drawbacks one could exert a priori, is outlined in Table 1. The HRR and HRRS allow a direct comparison of the quality of radar rainfall to the daily gauge data (DGR) that is available, whereas the hourly products (HRR and HRRS) allow an assessment of whether the scaling logic results in an improvement of the radar rainfall at finer timescales. Results of flow estimated using these three rainfall products were finally compared for their accuracy and effectiveness in the context of flood forecasting.

The next section describes the study area and data collection, followed by a description of the unified river basin simulator (URBS), the rainfall-runoff model used for runoff estimation. The methodology for estimating the three rainfall products is discussed next, followed by a description of the application of the URBS model for runoff estimation and an evaluation of simulated runoff hydrographs using the various rainfall inputs. Finally, the conclusions from the study are drawn in the last section.

Study Area and Data Collection

Study Area

The study area is the upper Ping River Basin, which is situated between latitude 17°14′30″ to 19°47′52″ N, and longitude 98°4′30″ to 99°22′30″ E in northern Thailand (Fig. 1). It covers the area of approximately 25,370 km^2 across the provinces of Chiang Mai and Lam Phun. Approximately 80% of the basin is mountainous. The basin landform ranges from an undulating to a rolling terrain. The Ping River originates in the Chiang Dao District in the north of Chiang Mai and flows downstream to the south to become the inflow for the Bhumiphol Dam, which is a large dam in Doi Tao District in Chiang Mai and has an active storage capacity of 9.7 billion m^3. The average annual rainfall and runoff of the catchment are approximately 1,170 and 270 mm, respectively.

Radar Reflectivity Data

Radar reflectivity data recorded from the Omkoi radar, owned and operated by the Bureau of Royal Rainmaking and Agricultural Aviation (BRRAA), was used for radar rainfall estimation in the study subcatchments of the upper Ping River Basin. The Omkoi radar is an S-band Doppler radar which transmits radiation with a wavelength of 10.7 cm and produces a beam width of 1.2°. After preprocessing, the used radar reflectivity data are provided in a Cartesian grid of 480 × 480 km extent with a 1-km^2 spatial resolution and 6-min temporal resolution. The radar reflectivity data provided by the BRRAA are pseudo-CAPPI reflectivities derived from the 2.5-km constant altitude plan position indicator (CAPPI) data at a range within 135 km from the radar site, from the lowest plan position indicator (PPI) (0.6°) beyond the 136 km range.

Reflectivity, gauge rainfall, and runoff data recorded at the same period were required for the analysis of this study. Three 2.5-km pseudo-CAPPI reflectivity data sets from the Omkoi radar during the rainy seasons for three years (June–October 2003, May–September 2004, and May–July 2005) were used in this study.

Because S-band reflectivity data were used in this study, beam attenuation was assumed to be insignificant (Hitschfeld and Bordan 1954; Delrieu et al. 2000). To avoid the effect of bright band and different observation altitude in the measured radar reflectivity, the pseudo-CAPPI reflectivity data that lie within the range where the height of the base scan beam center (0.6°) is below the climatological freezing level of Chaing Mai [approximately 4.9 km, according to Silverman and Sukarnjanaset (2000)] was used in the analysis. The maximum observation range that gives the height of the base scan beam center below the freezing level of 4.9 km is approximately 160 km. Thus, only reflectivity data that lie within 160 km of the radar were used in the analysis. Consequently, the reflectivity data used in this study were considered to be free from the effects of bright band and different observation altitudes.

To avoid the effect of noise and hail in the measured radar reflectivity, reflectivity values less than 15 dBZ were assumed to represent a reflectivity of 0 mm^6 m^{-3}, and those greater than 53 dBZ were assumed to equal 53 dBZ. Because the study area is mountainous, the errors attributable to the effect of ground clutter, beam blocking, and variations in the vertical profile of reflectivity (VPR) are potentially important. The effect of ground clutter and beam blocking were addressed by finding the clutter locations, where high persistence in the reflectivity is exhibited, blocking this area from the radar map, and then replacing the blocked locations with interpolated data from surroundings pixels that are not affected by clutter and beam blocking. Although variations in the VPR can impact the estimation of radar rainfall (Chumchean et al. 2008), lack of information about the VPR required the assumption that its impact was not systematic and would not impact the conclusions this study sought to draw.

Table 1. Summary of the Rainfall Data Products Evaluated

Rainfall product	Rationale	Benefits and drawbacks
DGR	Spatially averaged daily gauge rainfall, assessed at both daily and hourly scales (hourly transformation performed using equal hourly depths)	Use of crude disaggregation scheme to hourly is likely to lead to smaller peaks in resulting flood hydrograph; daily results expected to result in accurate outputs except for their inability to pick subdaily peaks
HRR	Using the same Z–R parameters based on daily gauge data and then accumulated into hourly radar rainfall	The use of hourly radar rainfall offers a big improvement in the subdaily temporal representation compared with the daily gauge rainfall product
HRSS	Same as HRR, except that the radar parameters are scaled to an hourly time step using the transformation function proposed by Mapiam et al. (2009)	Application of more suitable Z–R parameters than HRR can lead to improvement of the accuracy on hourly radar rainfall estimates and the resulting flow hydrographs

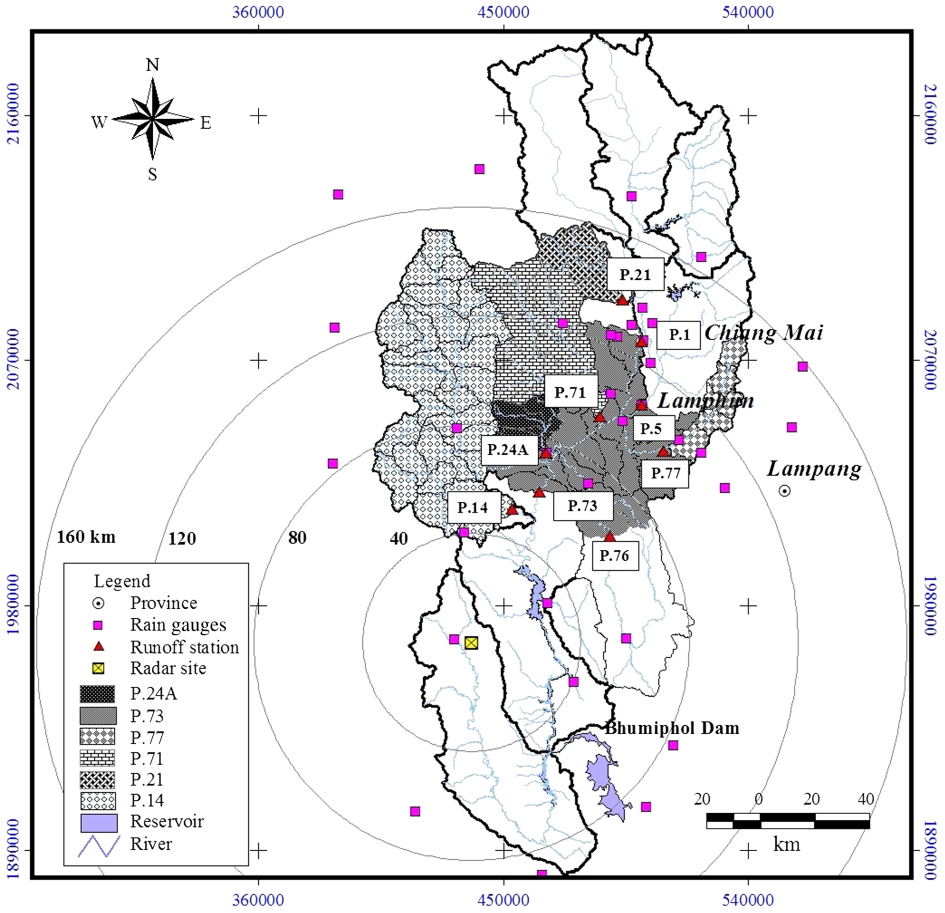

Fig. 1. The upper Ping River Basin and the locations of the radar, rain gauges, and runoff stations in the universal transverse mercator (UTM) coordinate system

Ground Rainfall Data

There are 35 rain gauges located within 160 km of the Omkoi radar. These rain gauges are owned and operated by the Royal Irrigation Department (RID) and the Thai Meteorological Department (TMD). Thirty-two stations are nonautomatic stations that provide daily rainfall data, whereas only three rain gauges are automatic stations. Because most of the gauges located inside and around the project area are daily rain gauges, three sets of daily rain-gauge rainfall data obtained from the network of 35 gauges for the same period as the reflectivity data were used in this study. Quality control of these rain-gauge rainfall data was performed by considering rainfall data from adjacent gauges and ensuring consistency in the ensuing double mass curves. If unusual rainfall data were found, these were excluded from the analysis.

Runoff Data

Continuous runoff data recorded from the six runoff stations located in the upper Ping River Basin—P.21, P.71, P.14, P.24A, P.77, and P.73—were used for model implementation in this study. These stations are located within 160 km of the Omkoi radar, and they have the catchment areas of 510, 1,727, 3,853, 454, 544, and 2,242 km^2, respectively. P.73 is actually the most downstream of the runoff stations P.1, P.5, P.71, P.77, P.76, and P.24A of the study area with the whole catchment area of approximately 12,910 km^2. To avoid error in radar rainfall estimates resulting from the effects of bright band and different observation altitudes, only a partial catchment area of the P.73 (2,242 km^2) located within the 160 km radar range (excluding the area of upstream runoff stations P.1, P.5, P.71, P.77, P.76, and P.24A) were therefore considered in the rainfall-runoff process in the study. Continuous runoff data from its five upstream stations were also collected to be used as inflow data during model simulation on P.73. All the runoff stations used in the analysis are owned and operated by the RID. The instantaneous runoff data at all stations collates flows on an hourly basis, at the same periods as the reflectivity and rain-gauge rainfall data, which were used in the analysis presented subsequently.

URBS Model

The unified river basin simulator (URBS) developed by Carroll (2007) was chosen for runoff simulation for the current study. URBS is a semidistributed nonlinear rainfall runoff routing model that can account for the spatial and temporal variation of rainfall. This model is based on research by Laurenson and Mein (1990) and has been used extensively for flood forecasting by the Australian Bureau of Meteorology and by the Chiangjiang (Yangtze) Water Resources Commission in China (Malone et al. 2003; Jordan et al. 2004). In the context of the study region, Mapiam and Sriwongsitanon (2009) used the URBS model for flood estimation on the gauged catchments in the upper Ping River Basin and later formulated some relationships for use on the ungauged catchments of the basin.

The Split module—a runoff routing module of the URBS model—was individually used for runoff estimation for the six runoff stations (P.21, P.71, P.14, P.24A, P.77, and P.73). The hypothesis of the Split module is that the rainfall excess on a subcatchment,

estimated by rainfall-runoff–loss models, is routed through the catchment storage, located at the centroid of that subcatchment, to the channel using a catchment routing relationship. Thereafter, outflow from the catchment storage, which is the inflow of channel storage (Q_u), will be routed along a reach (distance from the centroid to the outlet of the corresponding subcatchment) to the next downstream subcatchment, using the Muskingum method. In this study, flow components of the catchment and channel routing were calculated by using simplified equations as shown in Eqs. (1) and (2), respectively [see Carroll (2007) for the details on full equations]

$$S_{\text{catch}} = \beta\sqrt{A}Q^m \tag{1}$$

where S_{catch} = catchment storage (m^3s^{-1} h) of each subcatchment; β = catchment lag parameter (h/km) for each subcatchment; A = area of subcatchment (km^2); m = dimensionless catchment nonlinearity parameter; and Q = outflow of catchment storage (m^3/s) of the corresponding subcatchment

$$S_{\text{chnl}} = \alpha L[xQ_u + (1-x)Q_d] \tag{2}$$

where S_{chnl} = channel storage (m^3s^{-1} h) for each subcatchment; α = channel lag parameter (h/km) for each subcatchment; L = length of a reach (km) considered in channel routing; Q_u = inflow at upstream end of a reach [includes subcatchment inflow, Q, calculated using Eq (1)]; Q_d = outflow at downstream end of a channel reach (m^3s^{-1}) of the corresponding subcatchment; and x = Muskingum translation parameter.

The excess rainfall estimation on each subcatchment was calculated using the initial loss-proportional runoff model (IL-PR) for pervious area and the spatial infiltration model for impervious area assessment. The assumption of the IL-PR model is that the accumulated rainfall depth starting from the beginning of a simulation period (R_i) will be deducted by an initial loss (mm) until the R_i exceeds the maximum initial loss (IL in mm). The proportional loss using proportional runoff coefficient (pr, dimensionless) will later be applied for an assessment. The pervious excess rainfall depth at time t (R_t^{per}) is given by

$$R_t^{\text{per}} = \begin{cases} 0 & \text{if } R_i \le \text{IL} \\ (R_i - \text{IL}) - (1-\text{pr})(R_i - \text{IL}) & \text{if } R_i > \text{IL and } il_{i-1} < \text{IL} \\ (R_i - R_{i-1}) - (1-\text{pr})(R_i - R_{i-1}) & \text{if } R_i > \text{IL and } il_{i-1} = \text{IL} \end{cases} \tag{3}$$

$$R_i = R_t^{\text{tot}} + R_{i-1} \tag{4}$$

where R_t^{tot} = rainfall depth during a time interval (Δt), which is 1 hour in this study. The accumulated initial loss at time t (il_i), can be described as

$$il_i = \begin{cases} R_i & \text{if } R_i \le \text{IL} \\ \text{IL} & \text{if } R_i > \text{IL} \end{cases} \tag{5}$$

The effective fraction of the area that is impervious (f_{eff}) is given by Eq. (6)

$$f_{\text{eff}} = f_u + \frac{F_t}{F_{\max}}, \qquad \text{Max}(f_{\text{eff}}) = 1 \tag{6}$$

where f_u = existing fraction of the impervious area ($f_u = 0$ is assumed for this study); F_t = cumulative infiltration into the pervious area starting from the beginning of a simulation period; and $F_{\max}$ = maximum infiltration capacity of the subcatchment (IF parameter).

Excess rainfall (R_t) at time t on the corresponding subcatchment can be calculated using Eq. (7)

$$R_t = f_{\text{eff}}C_{\text{imp}}R_t^{\text{tot}} + (1-f_{\text{eff}})R_t^{\text{per}} \tag{7}$$

where C_{imp} = impervious runoff coefficient (the default is 1); and R_t^{per} = calculated using the IL-PR model.

As the URBS model equations have been simplified, there are seven model parameters necessary for the application. These parameters are: (1) the channel lag parameter (α); (2) the catchment nonlinearity parameter (m); (3) the Muskingum translation parameter (x); (4) the catchment lag parameter (β); (5) the initial loss (IL); (6) the proportional runoff coefficient (PR); and (7) the maximum infiltration rate (IF). However, as the parameters m and x do not vary significantly from 0.8 and 0.3, respectively (Carroll 2007; Jordan et al. 2004), both parameters were fixed at these values in our study. As a result, only five model parameters were necessary to specify on each subcatchment for further application in the study. The parameters α and β are related to the runoff routing behavior, and the parameters IL, PR, and IF are related to rainfall loss estimation.

To implement the URBS model for runoff estimation, the catchments corresponding to runoff stations P.21, P.71, P.14, P.24A, P.77, and P.73 (Fig. 1) were divided into a number of subcatchments (5, 15, 25, 5, 5, and 14, for each of the preceding main subcatchments, respectively). Each subcatchment was selected so as to have similar size (sizes varied between 90 and 160 km^2) and characteristics. For each runoff station, the total rainfall for each subcatchment was estimated using three alternatives as described subsequently. The total rainfall and a set of model parameters associated with each subcatchment were then used to simulate the runoff hydrograph at the corresponding runoff station. Based on an assumption of the URBS model, it is necessary to define the five model parameters on each subcatchment. However, because there is no runoff station located in other upstream subcatchments of the six runoff stations, this becomes a difficult task. Consequently, all subcatchments of each runoff station are considered to have a uniform set of parameters. These model parameters can be, and are usually, obtained by model calibration as explained in "Assessment of Model Parameters."

Catchment Rainfall Estimation

Three products of catchment rainfall (DGR, HRR, and HRRS) for the three periods were ascertained to serve as the input data for the URBS model for runoff estimation at the six runoff stations. The products of daily rainfall (DGR) were assessed at both a daily timescale and also disaggregated to hourly by considering constant hourly rain rates along the day before inputting into the URBS model. The calculated rainfall during June–October 2003 was used for model calibration, and May–September 2004 and May–July 2005 were used for model verification. Methods used for catchment rainfall estimation are explained next.

Estimation of Daily Gauge Rainfall

Rain gauge rainfall data has generally been used to estimate areal rainfall and then used as the input data to a rainfall-runoff model for runoff and flood estimation. The DGR was spatially averaged using the Thiessen polygon approach (Chow et al. 1988; Bae et al. 2008) over the study region to form the first of the rainfall input alternatives evaluated. Jiang et al. (2007) suggested that although many methods are available for estimating mean areal rainfall such as splines (regularized and tension), inverse distance weighting

(IDW), trend surface, and kriging, Thiessen polygon approach has been selected for estimating mean areal rainfall over application areas such as the Dongjiang Basin in south China. This is primarily because this approach is probably the most common approach for modeling the spatial distribution of rainfall and it is known to provide good results when used for relatively dense networks (Naoum and Tsanis 2004). The approach has been widely used in many applications (Panigrahy et al. 2009; Bhat et al. 2010), including for radar rainfall estimation (Wu et al. 2008). Furthermore, as the model used in this study requires rainfall inputs at the subcatchment level (and not at a pixel level), the added sophistication of the grid-based rainfall interpolation approaches is not considered warranted.

In this research, 35 daily rain gauges located within and around the upper Ping River Basin were used to construct the Thiessen polygons. DGR for each subcatchment was calculated by multiplication of the daily gauge rainfall and its corresponding weighting factor from the associated polygon.

Estimation of Hourly Radar Rainfall

Various forms of Z–R relationships ($Z = AR^b$) for ascertaining radar rainfall have been suggested in the literature (Marshall and Palmer 1948; Joss and Waldvogel 1970; Battan 1973; Atlas et al. 1999; Uijlenhoet et al. 2003; Lee and Zawadzki 2005). However, these relationships cannot be directly applied in all regions because the A and b parameters of the Z–R relationship vary depending on many factors, including their dependence on the rainfall drop size distribution (DSD), which varies in both space and time. Typical values of the multiplicative term A may range from 31 to 500 (Battan 1973; Seed et al. 1996, 2002; Steiner et al. 1999), whereas the exponent b varies from 1 to 3 (Smith and Krajewski 1993), with typical values between 1.2 and 1.8 (Battan 1973; Ulbrich 1983). Because daily rain-gauge rainfall data are the finest resolution available in the upper Ping River Basin, Mapiam and Sriwongsitanon (2008) then developed a climatological Z–R relationship ($Z = 74R^{1.6}$) based on daily data for radar rainfall estimation in the upper Ping River Basin. This equation is unavoidably used to assess radar rainfall at finer resolution than the available gauge data.

To assess HRR, the daily Z–R relationship ($Z = 74R^{1.6}$) was used to convert three instantaneous radar reflectivity data sets of the Omkoi radar into instantaneous radar rainfall intensity. This derived instantaneous radar rainfall at all pixels located in the six gauged catchments was then accumulated into HRR by using the accumulation method proposed by Fabry et al. (1994). The HRR for each subcatchment was estimated by averaging radar rainfall of all pixels located within a considered subcatchment, using a simple arithmetic averaging method.

Estimation of Hourly Radar Rainfall using the Scaling Transformation Equation

The A parameter of the Z–R relationship tends to decrease with a decrease in the rainfall temporal resolution used to develop the relationship. Application of daily (24-h) Z–R relationship to estimate radar rainfall at finer temporal resolutions, especially at hourly scale, can give significant error on extreme rainfall estimates (Mapiam et al. 2009). To reduce this error, Mapiam et al. (2009) proposed a climatological scaling transformation equation for converting the A parameter that was calibrated using daily data to finer resolutions as

$$A_t = \left(\frac{t}{24}\right)^{-0.055} A_{24} \tag{8}$$

where $t/24$ = scale factor; t (h) = temporal resolution at which the rainfall needs to be estimated; 24 (h) = reference temporal resolution of the radar rainfall; 0.055 = scaling exponent; and A_{24} and A_t represent the parameter A in Z–R relationship at 24- and t-h resolutions, respectively.

From the results of Mapiam et al. (2009), it was evident that the proposed scale- transformed equation of the Z–R relationship was valid for the S-band radar and also exhibited significant improvements in estimating extreme rainfall at finer temporal resolutions. Therefore, the proposed scaling transformation equation in Eq. (8) was used to estimate a scale-transformed hourly A parameter. The scale-transformed hourly A parameter (A_1) was estimated as

$$(A_1) = \left(\frac{1}{24}\right)^{-0.055} (A_{24}) \tag{9}$$

The estimated scale-transformed hourly Z–R relationship ($Z = 88R^{1.6}$) was used to convert instantaneous reflectivity data into rainfall rate; thereafter, the instantaneous radar rainfall was accumulated into an HRRS using the Fabry et al. (1994) method.

Application of the URBS Model for Runoff Estimation

Assessment of Model Parameters

The URBS model was used to estimate hourly runoff hydrograph at six runoff stations (P.21, P.71, P.14, P.24A, P.77, and P.73) by using three rainfall products (DGR, HRR, and HRRS) as the input data. One data set of radar reflectivity and rain-gauge data during June–October 2003 were used in the model calibration (Fig. 2 is an example of a time series of the three rainfall products at the runoff station P.14). Model parameters of each runoff station were therefore analyzed individually for each rainfall product using the model calibration process. Model calibration was carried out by adjusting the five model parameters (α, β, IL, PR, and IF) until the optimal fit between the observed and calculated hydrographs at each runoff station was satisfied.

To reach the optimal set of model parameters corresponding to each rainfall product at each runoff station, a grid-based parameter search was used. The detailed methodology is described as follows:

1. Specify a uniform assessment point of each model parameter covering the associated range for each grid to be used for the URBS model simulation as presented in Table 2. In this research, 21,870 parameter combinations were assessed at each runoff station.

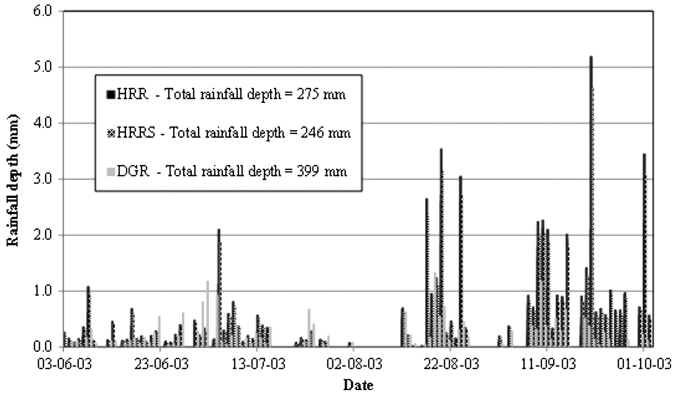

Fig. 2. Comparison of the three hourly rainfall products for the runoff station P.14 during the calibration period

Table 2. Model Parameter Values Used for Creating 21,870 Parameter Combinations for Model Calibration

Runoff station using the parameters	Model parameter values used in calibration process				
	α	β	IL (mm)	PR	IF (mm)
P.21, P.71, P.77,	0.1	5	0	0.05	700
P.24A, and P.14	0.2	6	10	0.07	800
—	0.3	7	20	0.09	900
—	0.4	8	30	0.11	1,000
—	0.5	9	40	0.13	1,100
—	0.6	—	50	0.15	1,200
—	—	—	60	0.17	1,300
—	—	—	80	0.19	1,400
—	—	—	100	0.21	1,500
P.73	0.1	5	0	0.19	300
—	0.2	6	10	0.21	400
—	0.3	7	20	0.23	500
—	0.4	8	30	0.25	600
—	0.5	9	40	0.27	700
—	0.6	—	50	0.29	800
—	—	—	60	0.31	900
—	—	—	80	0.33	1,000
—	—	—	100	0.35	1,100

2. By using each rainfall product as the input data for each runoff station, every parameter set was individually applied to the URBS model to estimate the hourly flow hydrographs. Overall root mean square error (RMSE) between the calculated and measured discharges for each simulation case was then assessed using the following:

$$\text{RMSE} = \left(\frac{\sum_{i=1}^{N} (Q_{m,i} - Q_{c,i})^2}{N} \right)^{0.5} \quad (10)$$

where $Q_{m,i}$ denotes the observed discharge at time i; $Q_{c,i}$ = calculated discharge at time i; and N = number of data points.

3. Estimate the optimal parameter set for each rainfall product at each runoff station evaluated by minimizing the RMSE for all simulation cases.

Table 3. Model Parameters for Six Runoff Stations and Three Rainfall Products

Runoff station	Rainfall product	Control parameters for the URBS model				
		α	β	IL	PR	IF
P.21	DGR	0.5	5	40	0.07	700
	HRR	0.5	6	0	0.17	700
	HRRS	0.5	6	0	0.19	700
P.71	DGR	0.5	9	100	0.05	700
	HRR	0.3	5	50	0.13	700
	HRRS	0.3	5	50	0.17	900
P.77	DGR	0.1	8	80	0.09	1,500
	HRR	0.4	6	0	0.05	1,200
	HRRS	0.5	6	10	0.07	1,200
P.24A	DGR	0.5	9	60	0.17	700
	HRR	0.2	5	10	0.09	1,400
	HRRS	0.2	5	10	0.11	1,300
P.73	DGR	0.1	8	30	0.23	700
	HRR	0.2	5	30	0.31	500
	HRRS	0.2	5	30	0.33	500
P.14	DGR	0.2	8	100	0.09	1,200
	HRR	0.1	6	0	0.17	1,500
	HRRS	0.1	5	0	0.19	1,500

Table 4. RMSE during the Calibration and Verification Periods for Each Runoff Station and Each Rainfall Product

Runoff station	Rainfall product	RMSE (m^3/s)		
		Calibration period	Verification period	
		(2003)	(2004)	(2005)
P.21	DGR	2.710	4.678	3.019
	HRR	3.465	3.547	4.320
	HRRS	3.479	3.462	3.826
P.71	DGR	7.280	9.946	15.696
	HRR	6.271	11.349	14.409
	HRRS	6.265	10.959	14.559
P.77	DGR	1.818	2.816	4.535
	HRR	1.521	2.793	4.627
	HRRS	1.516	2.809	4.645
P.24A	DGR	2.760	4.230	3.980
	HRR	2.370	4.063	2.955
	HRRS	2.365	4.060	3.068
P.73	DGR	59.504	51.470	39.441
	HRR	51.963	65.590	55.718
	HRRS	53.823	58.523	47.307
P.14	DGR	12.745	22.342	37.434
	HRR	15.608	36.206	22.156
	HRRS	15.368	34.879	22.101

The results of model calibration explicitly show that the model parameters change with rainfall products (depending upon the rainfall depths and their distribution) and runoff station as presented in Table 3. According to the results, which show high variations between ground and radar rainfall products (e.g., Fig. 2) resulting in significant differences of model parameters between the DGR and the HRR and HRRS. On the other hand, smaller differences of the model parameters exist between HRR and HRRS because the distribution of these rainfall products is the same but the difference is only that the depth of HRR is higher than HRRS by the factor of approximately 1.12 (caused by the scaled Z–R relationship).

By using these calibrated parameters for runoff estimation for the chosen flow periods, the outcomes of model calibration identified by RMSE for each runoff station and each rainfall product are summarized in Table 4. Fig. 3 illustrates the time series plots comparing the observed and calculated flow hydrographs using different rainfall products at the runoff station P.24A. A comparison on runoff accuracy in model applications using different rainfall products are discussed in "Evaluation of Simulated Runoff Hydrographs Using Alternate Rainfall Inputs."

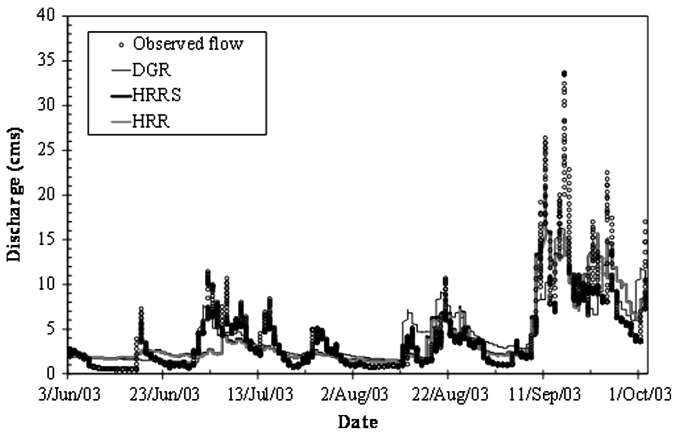

Fig. 3. Comparison of hourly observed and calculated flow hydrographs at the runoff station P.24A during the calibration period

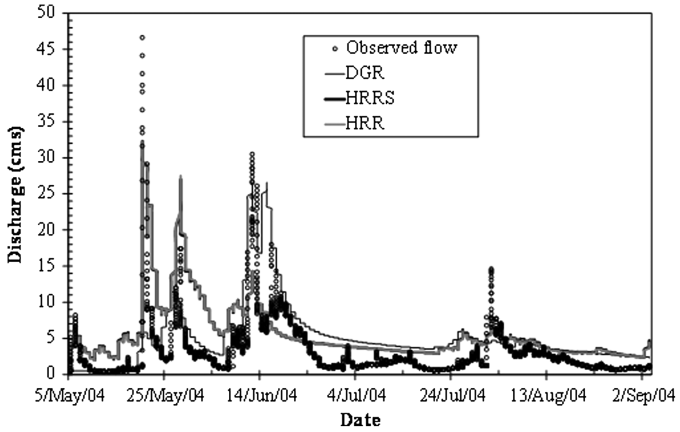

Fig. 4. Comparison of hourly observed and calculated flow hydrographs at the runoff station P.24A during the verification period

Verification of the Calibrated Model Parameters

The verification process was carried out in this study to provide more data sets to be used for the comparison of the accuracy among different rainfall products and to ensure that the same data set of the calibrated model parameters can be applied for other rainfall events. Data during the periods May–September 2004 and May–July 2005 were used for an assessment. Results of RMSE between the calculated and measured discharges for each runoff station and each rainfall product during these two periods are also summarized in Table 4, which shows that the accuracy of the calculated flow hydrographs for the verification period reduce compared with the results gained during the calibration period as shown by increasing RMSE values. This is to be expected because model parameters for the verification process cannot be changed to minimize RMSE between the calculated and measured discharges for each simulation case. Selected time series plots comparing hourly observed and calculated flow hydrographs during the verification period in 2004 at runoff station P.24A are presented in Fig. 4.

Evaluation of Simulated Runoff Hydrographs Using Alternate Rainfall Inputs

The three rainfall alternatives to be used as inputs were evaluated for the simulation of flow hydrographs over the upper Ping River Basin. Within those three rainfall inputs, any rainfall product that can simulate a flow hydrograph closest to the observed hydrograph was defined as the most suitable. To accomplish this objective, the model structure (including model parameters) for each rainfall product was kept the same; then the rainfall input was changed to observe the differences that resulted. To ensure an unbiased outcome from the study, the model evaluation was performed using each set of model parameters to simulate three sets of flow hydrographs using the three rainfall products as the input data. Hence, the model was run 3×3 (nine) times for each runoff station and each data period. The RMSE was the statistical measure to evaluate the accuracy of the overall hydrograph for each simulation case. A summary of the performance of all simulation cases is presented in Table 5, which shows that for the overall 54 simulation cases, there are 31 (57%), 12 (33%), and 11 (31%) cases of the HRRS, HRR, and DGR, respectively, that can produce the minimum RMSE among each case. The Table 5 also presents the total average of the RMSE of each rainfall product for all parameter sets and simulation periods (RMSE on the same row). It shows five runoff stations (P.21, P.71, P.77, P.73, and P.14) where HRRS provided the minimum RMSE. Only at the runoff station P.24A is the minimum RMSE produced by DGR, but its RMSE is very close to that produced by HRRS (3.439 and 3.616, respectively). On the other hand, there are four runoff stations (P.21, P.71, P.73, and P.14) where DGR provided the maximum RMSE. There are only two runoff stations (P.77 and P.24A) where the maximum RMSE is produced by HRR. Table 5 also shows the percentage increment of the average RMSE from the minimum RMSE of any rainfall product at

Table 5. Comparison of Model Performance in Runoff Estimation Using Three Different Rainfall Products

Gauge station	Rainfall product	RMSE (m^3/s) of each parameter set used for flow simulation									Total average	Increment of average RMSE from the minimum RMSE (%)
		Calibration period			Verification period							
		2003			2004			2005				
		DGR	HRR	HRRS	DGR	HRR	HRRS	DGR	HRR	HRRS		
P.21	DGR	2.710	4.848	5.528	4.678	8.504	9.364	3.019	5.435	6.141	*5.581*	*55*
	HRR	4.398	3.465	3.508	3.763	3.547	3.811	2.249	4.320	5.033	3.788	5
	HRRS	4.673	3.532	3.479	4.068	3.342	3.462	2.670	3.267	3.826	**3.591**	**0**
P.71	DGR	7.280	15.648	18.825	9.946	20.248	23.530	15.696	31.760	36.002	*19.882*	*118*
	HRR	10.614	6.271	6.727	7.211	11.349	13.488	4.578	14.409	17.548	10.244	12
	HRRS	11.711	6.545	6.265	7.603	9.239	10.959	3.614	11.689	14.559	**9.132**	**0**
P.77	DGR	1.818	2.036	1.968	2.816	2.209	2.791	4.535	3.960	4.654	2.976	6
	HRR	1.762	1.521	1.614	2.790	2.793	3.315	5.462	4.627	5.605	*3.277*	*16*
	HRRS	1.709	1.621	1.516	2.280	2.412	2.809	4.505	3.823	4.645	**2.813**	**0**
P.24A	DGR	2.760	3.575	3.386	4.230	3.313	3.498	3.980	2.861	3.350	**3.439**	**0**
	HRR	4.650	2.370	2.501	7.762	4.063	4.798	5.192	2.955	3.609	*4.211*	*22*
	HRRS	3.798	2.488	2.365	6.379	3.548	4.060	4.269	2.574	3.068	3.616	5
P.73	DGR	59.504	63.192	61.256	51.470	65.391	67.391	39.441	62.888	63.475	*59.334*	*15*
	HRR	58.464	51.963	57.527	52.252	65.590	67.590	33.896	55.718	57.806	55.645	8
	HRRS	60.610	56.012	53.823	48.863	60.523	58.523	28.794	50.189	47.307	**51.627**	**0**
P.14	DGR	12.745	40.021	48.297	22.342	54.424	63.139	37.434	76.423	87.044	*49.097*	*101*
	HRR	29.280	15.608	16.378	23.450	36.206	40.967	22.857	22.156	24.535	25.715	5
	HRRS	31.536	16.018	15.368	23.427	31.055	34.879	24.580	20.523	22.101	**24.388**	**0**

Note: Stations where HRRS provided the minimum RMSE are indicated in bold font; stations where DGR provided the maximum RMSE are italic font.

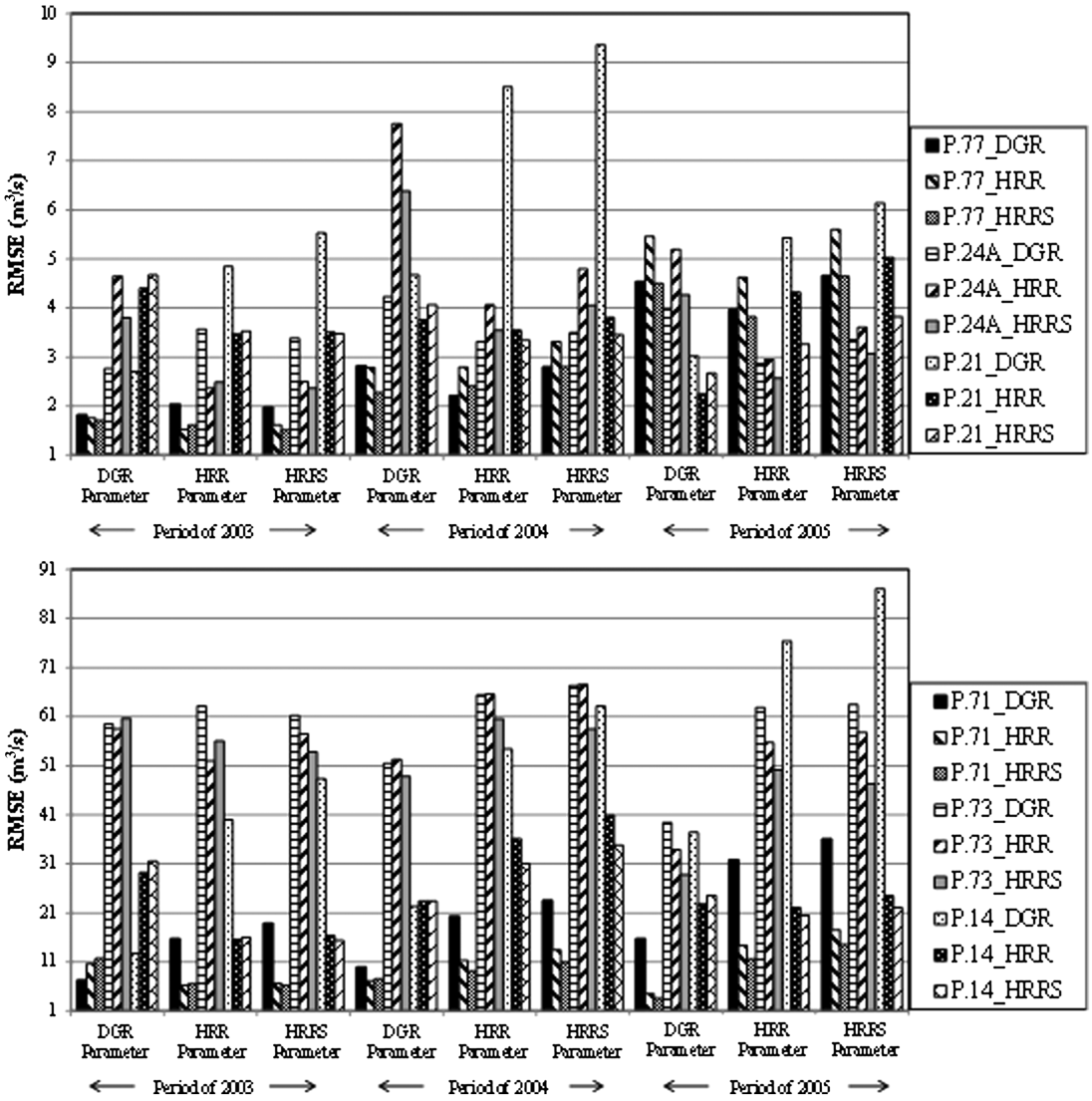

Fig. 5. Comparison of RMSE values of the three rainfall inputs for different simulation cases at the six runoff stations

each runoff station. At four runoff stations (P.21, P.71, P.73, and P.14), the DGR generated the increment percentage of approximately 55, 118, 15, and 101, respectively, which are quite high in most cases. On the other hand, there are two stations (P.77 and P.24A) where HRR generated a lower increment percentage of approximately 16 and 22, respectively, compared with the increment percentage that DGR generated. This is especially true for the HRRS that generated very little increment percentage of approximately 5% only at the runoff station P.24A. Finally, the comparison of RMSE values of the three rainfall inputs for different simulation cases at the six runoff stations is shown in Fig. 5, which presents the RMSE of each rainfall product for all parameter sets and simulation periods (RMSE on the same row) at each particular runoff station. Fig. 5 has confirmed that HRRS can generate a lower RMSE between the calculated and measured discharges for each simulation case compared with RMSE generated by HRR; this is especially the case with respect to that generated by DGR. The preceding results demonstrate that HRRS calculated by applying the scaling transformation equation to the daily *Z–R* relationship leads to the most appropriate rainfall data set for runoff simulation. This is a further validation of the scaling results that were presented by Mapiam et al. (2010), pointing to the need to further ascertain the specific reasons that lead to the scaling rule being applicable.

Conclusions

Radar rainfall data can provide higher spatial and temporal resolution compared with rain-gauge measurements (AghaKouchak et al. 2010). Such higher resolutions have been known to lead to improvements in the accuracy of the resulting runoff sequences. However, radar rainfall estimation requires continuous rain gauge rainfall data to calibrate and update the *Z–R* relationship, such data being usually unavailable in most of the developing world including the upper Ping River Basin in northern Thailand, the study area for this paper. In the absence of such data, the option that is usually used is to aggregate the radar rainfall to a daily timescale and derive the needed relationship using daily ground rainfall. This, however, has been shown to lead to biased rainfall in Mapiam et al. (2009), which presents a scaling rationale that allowed derivations of the *Z–R* relationship at a time scale different to that used in the calibration. The present paper uses this scaling rationale to modify the *Z–R* relationship calibrated using daily ground rainfall data to formulate a hourly rainfall product termed HRRS then verifies whether HRRS leads to improvements in ensuing hydrological applications if alternate rainfall inputs are used. Two additional rainfall products are assessed—the DGR and the HRR evaluated using the *Z–R* relationship calibrated from the daily gauge rainfall.

This assessment uses the URBS, a semidistributed rainfall-runoff model, to assess the relative benefits of using either of these three rainfall inputs. The accuracy of the overall flow hydrograph estimated using the two products of radar rainfall (HRRS and HRR) as inputs are explicitly higher than that using DGR. This result is a likely artifact of the size of the catchment and the relatively sparse daily rain-gauge network that is available to sample the daily rainfall distribution. The insights gained in this study would provide more evidence alongside many other studies, which suggest that radar rainfall can be used effectively to represent more accurate rainfall product compared with rain-gauge rainfall (Johnson et al. 1999; Jayakrishnan et al. 2004; Waleed et al. 2009; Biggs and Atkinson 2011). In addition, HRRS demonstrates consistently accurate results in hourly runoff estimation of the overall flow hydrographs. Consequently, the scaling transformation used to derive the HRRS rainfall product appears to have merit in formulating continuous rainfall. It is expected that this transformation will be of considerable use in locations where radar rainfall relationships can only be calibrated against ground rainfall data measured at a daily resolution.

Acknowledgments

The first and the last authors gratefully acknowledge the Thailand Research Fund through the Royal Golden Jubilee Ph.D. program (Grant No. PhD/0118/2547) and the Kasetsart University Research and Development Institute for financially supporting this research. We also appreciate the BRRAA, RID, and TMD for providing the radar data and hydrological data used in this study. Finally, the authors would like to thank Dr. Siriluk Chumchean for her suggestions on radar rainfall estimation, and also to the anonymous reviewers, whose constructive comments have helped enhance the paper.

References

AghaKouchak, A., Habib, E., and Bárdossy, A. (2010). "Modeling radar rainfall estimation uncertainties: random error model." *J. Hydrol. Eng.*, 10.1061/(ASCE)HE.1943-5584.0000185, 265–274.

Anquetin, S., et al. (2010). "Sensitivity of the hydrological response to the variability of rainfall fields and soils for the Gard 2002 flash–flood event." *J. Hydrol.*, 394(1–2), 134–147.

Atlas, D., Ulbrich, C. W., Jr., Mark, F. D., Amitai, E., and Williams, C. R. (1999). "Systematic variation of drop size and radar-rainfall relation." *J. Geophys. Res.* 104(D6), 155–169.

Battan, L. J. (1973). *Radar observation of the atmosphere*, Univ. of Chicago Press, Chicago, 324.

Bae, Y. H., Kim, B. S., Seoh, B. H., Kim, H. S., and Kwon, H. H. (2008). "Radar rainfall adjustment by Kalman-filter method and flood simulation using two distributed models." *Proc., 5th European Conf. on Radar in Meteorology and Hydrology (ERAD)*, Finish Meteorological Institute, Helsinki, Finland.

Bhat, S., Jacobs, J. M., Hatfield, K., and Graham, D. (2010). "A comparison of storm-based and annual-based indices of hydrologic variability: A case study in Fort Benning, Georgia." *Environ. Monit. Assess.*, 167(1–4), 297–307.

Biggs, E. M., and Atkinson, P. M. (2011). "A comparison of gauge and radar precipitation data for simulating an extreme hydrological event in the Severn Uplands, UK." *Hydrol. Process.*, 25(5), 795–810.

Borga, M., Anagnostou, E. N., and Enrico, F. (2000). "On the use of realtime radar rainfall estimates for flood prediction in mountainous basins." *J. Geophys. Res.*, 105(D2), 2269–2280.

Carroll, D. G. (2007). *URBS: A rainfall runoff routing model for flood forecasting and design version 4.30, user manual*, Queensland Dept. of Natural Resources and Mines, QLD, Australia, 160.

Chow, V. T., Maidment, D. R., and Mays, L. W. (1988). *Applied hydrology*, McGraw-Hill, New York.

Chumchean, S., Seed, A., and Sharma, A. (2006a). "Correcting of real-time radar rainfall bias using a Kalman filtering approach." *J. Hydrol.*, 317(1–2), 123–137.

Chumchean, S., Sharma, A., and Seed, A. (2006b). "An integrated approach to error correction for real–time radar–rainfall estimation." *J. Atmos. Oceanic Technol.*, 23(1), 67–79.

Chumchean, S., Sharma, A., and Seed, A. (2008). "An operational approach for classifying storms in real time radar rainfall estimates." *J. Hydrol.*, 363(1–4), 1–17.

Collier, C. G. (1996). *Applications of weather radar system: A guide to uses of radar in meteorology and hydrology*, Wiley, New York, 383.

Collinge, V. K., and Kirby, C. (1987). *Weather radar and flood forecasting*, Wiley, Chichester, U.K.

Doviak, R. J., and Zrnic, D. S. (1992). *Doppler radar and weather observation*, Academic Press, Orlando, FL, 545.

Delrieu, G., Andrieu, H., and Creutin, J. D. (2000). "Quantification of path-integrated attenuation for X- and C-band weather radar systems operating in Mediterranean heavy rainfall." *J. Appl. Meteorol*, 39(6), 840–850.

Fabry, F., Bellon, A., Duncan, M. R., and Austin, G. L. (1994). "High resolution rainfall measurements by radar for very small basins: The sampling problem reexamined." *J. Hydrol.*, 161(1–4), 415–428.

Hitschfeld, W., and Bordan, J. (1954). "Errors inherent in the radar measurement of rainfall at attenuating wavelengths." *J. Meteorol.*, 11(1), 58–67.

Jayakrishnan, R., Srinivasan, R., and Arnold, J. (2004). "Comparison of raingage and WSR-88D Stage III precipitation data over the Texas-Gulf basin." *J. Hydrol.*, 292(1–4), 135–152.

Jiang, T., Chen, Y. D., Xu, C., Chen, X., Chen, X., and Singh, V. P. (2007). "Comparison of hydrological impacts of climate change simulated by six hydrological models in the Dongjiang Basin, South China V.P." *J. Hydrol.*, 336(3–4), 316–333.

Johnson, D., Smith, M., Koren, V., and Finnerty, B. (1999). "Comparing mean areal precipitation estimates from NEXRAD and gauge networks." *J. Hydrol. Eng.*, 10.1061/(ASCE)1084-0699(1999)4:2(117), 117–124.

Jordan, P., Seed, A., May, P., and Keenan, T. (2004). "Evaluation of dual polarization radar for rainfall runoff modeling–A case study in Sydney, Australia." *6th Int. Symp. on Hydrological Applications of Weather Radar*, Bureau of Meteorology, Melbourne, Australia.

Joss, J., and Waldvogel, A. (1970). "A method to improve the accuracy of radar measured amounts of precipitation." *14th Radar Meteorology Conf.*, American Meteor Society, Tucson, AZ, 237–238.

Krajewski, W. F., and Smith, J. A. (2002). "Radar hydrology: Rainfall estimation." *Adv. Water Resour.*, 25(8), 1387–1394.

Laurenson, E. M., and Mein, R. G. (1990). *RORB–version 4, runoff routing program user manual*, Dept of Civil Engineering, Monash Univ., Monash, Victoria, Australia.

Lee, G. W., and Zawadzki, I. (2005). "Variability of drop size distribution: Time-scale dependence of the variability and its effects on rain estimation." *J. Appl. Meteorol.*, 44(2), 241–255.

Malone, T., Johnston, A., Perkins, J., and Sooriyakumaran, S. (2003). "Australian Bureau of Meteorology, HYMODEL—A real-time flood forecasting system." *Int. Hydrology and Water Resources Symp.*, Institution of Engineers, Barton, Canberra, Australia.

Mapiam, P. P., and Sriwongsitanon, N. (2008). "Climatological *Z–R* relationship for radar rainfall estimation in the upper Ping River Basin." *ScienceAsia J.*, 34(2), 215–222.

Mapiam, P. P., and Sriwongsitanon, N. (2009). "Estimation of the URBS model parameters for flood estimation of ungauged catchments in the upper Ping River Basin, Thailand." *ScienceAsia. J.*, 35(1), 49–56.

Mapiam, P. P., Sriwongsitanon, N., Chumchean, S., and Sharma, A. (2009). "Effect of rain-gauge temporal resolution on the specification of a Z-R relationship." *J. Atmos. Oceanic Technol.*, 26(7), 1302–1314.

Marshall, J. S., and Palmer, W. M. (1948). "The distribution of raindrops with size." *J. Meteorol.*, 5(4), 165–166.

Morin, E., Jacoby, Y., Navon, S., and Bet-Halachmi, E. (2009). "Towards flash flood prediction in the dry Dead Sea region utilizing radar rainfall information." *Adv. Water Resour.*, 32(7), 1066–1076.
Naoum, S., and Tsanis, I. K. (2004). "Ranking spatial interpolation techniques using a GIS-based DSS." *Global NEST J.*, 6(1), 1–20.
Panigrahy, N., Jain, S. K., Kumar, V., and Bhunya, P. K. (2009). "Algorithms for computerized estimation of Thiessen weights." *J. Comput. Civ. Eng.*, 10.1061/(ASCE)0887-3801(2009)23:4(239), 239–247.
Pessoa, M. L., Rafael, L. B., and Earle, R. W. (1993). "Use of weather radar for flood forecasting in the Sieve river basin: A sensitivity analysis." *J. Appl. Meteorol.*, 32(3), 462–475.
Rinehart, R. E. (1991). *Radar for meteorologists*, Univ. of North Dakota Press, Grand Forks, ND, 333.
Seed, A., and Austin, G. L. (1990). "Sampling errors for rain gauge derived mean-areal daily and monthly rainfall." *J. Hydrol.*, 118(1), 163–173.
Seed, A., Nicol, W. J., Austin, G. L., Stow, C. D., and Bradley, S. G. (1996). "The impact of radar and rain gauge sampling errors when calibrating a weather radar." *Meteor. Appl.*, 3(1), 43–52.
Seed, A., Siriwardena, L., Sun, X., Jordan, P., and Elliott, J. (2002). "On the calibration of Australian weather radars." *Cooperative Research Centre for Catchment Hydrology, Tech. Rep. 02/7*, Melbourne, Australia, 40.
Segond, M., Wheater, H. S., and Onof, C. (2007). "The significance of spatial rainfall representation for flood runoff estimation: A numerical evaluation based on the Lee catchment, UK." *J. Hydrol.*, 347(1–2), 116–131.
Silverman, B. A., and Sukarnjanaset, W. (2000). "Results of the Thailand warm-cloud hygroscopic particle seeding experiment." *J. Appl. Meteorol.*, 39(7), 1160–1175.
Smith, J. A., and Krajewski, W. F. (1993). "A modeling study of rainfall rate–reflectivity relationships." *Water Resour. Res.*, 29(8), 2505–2514.
Steiner, M., Smith, J. A., Burges, S. J., Alonso, C. V., and Darden, R. W. (1999). "Effect of bias adjustment and rain gauge data quality control on radar rainfall estimation." *Water Resour. Res.*, 35(8), 2487–2503.
Sun, X., Mein, R. G., Keenan, T. D., and Elliott, J. F. (2000). "Flood estimation using radar and raingauge data." *J. Hydrol.*, 239(1–4), 4–18.
Uijlenhoet, R. (2001). "Raindrop size distributions and radar reflectivity-rain rate relationships for radar hydrology." *Hydrol. Earth Syst. Sci.*, 5(4), 615–627.
Uijlenhoet, R., Steiner, M., and Smith, J. A. (2003). "Variability of raindrop size distribution in a squall line and implication for radar rainfall estimation." *J. Hydrometeorol.*, 4(1), 43–61.
Ulbrich, C. W. (1983). "Natural variations in the analytical form of the raindrop size distribution." *J. Climate Appl. Meteor.*, 22(10), 1764–1775.
Vieux, B. E. (2003). *Combined use of radar and gauge measurements for flood forecasting using a physics-based distributed hydrologic model*, Vieux and Associates, Norman, OK.
Waleed, A. R. M., Amin, M. S. M., Halim, G. A., Shariff, A. R. M., and Aimrun, W. (2009). "Calibrated radar–derived rainfall data for rainfall–runoff modeling." *Eur. J. Sci. Res.*, 30(4), 608–619.
Wu, T. S., Gilbert, D., Fuelberg, H. E., Cooper, H., Bottcher, D., and Reed, C. (2008). "Doppler radar-derived rainfall data monitoring to support surface water modeling of TMDL." *J. Coastal Res.*, 2008(10052), 273–280.
Wyss, J., Williams, E. R., and Bras, R. L. (1990). "Hydrologic modelling of New England river basins using radar rainfall data." *J. Geophys. Res.*, 95(D3), 2143–2152.
Yang, D., Koike, T., and Tanizawa, H. (2004). "Application of a distributed hydrological model and weather radar observations for flood management in the upper Tone River of Japan." *Hydrol. Process.*, 18(16), 3119–3132.